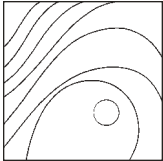


Histologic and Immunohistochemical Description of Early Healing at Marginal Defects Around Implants



Daniela Carmagnola, DDS, PhD¹/Daniele Botticelli, MD, PhD²
 Elena Canciani, MS, PhD³/Fabio Rossi, DDS, PhD⁴
 Stefano Milani, DDS, PhD³/Claudia Dellavia, DDS, PhD⁵

This study reports on the histologic characteristics of the early phases of implant osseointegration, focusing on osteopontin concentrations in the coronal area of implants placed with marginal defects and in control sites without defect preparation. In the mandibular right area of 12 dogs, two recipient sites were prepared and the margins were widened to obtain a gap of 0.5 mm at one site (small defect) and 1.25 mm at another site (large defect). Implants were placed and allowed a fully submerged healing. The procedure was subsequently performed in the left side in such a way as to obtain healing times of 5, 10, 20, and 30 days. Paraffin sections were stained with osteopontin antibodies and analyzed. At control implants, scarcely organized collagen fibers were observed in the space between the pristine bone and implant and were quickly replaced by mineralized tissue. In the small and large defects, the collagen fibers were organized in a layer that ran parallel to the implant at day 10 and became denser and thicker with time. Osteopontin was evenly distributed in the peri-implant tissue at control implants, while it was mainly located in the collagen bundle section around the implants placed in the defects. (Int J Periodontics Restorative Dent 2014;34:e50–e57. doi: 10.11607/prd.1786)

Osseointegration of oral implants has been proposed to occur with two different patterns.¹ Following the establishment of a blood fibrin clot in the gap between the pristine bone and the implant surface, vascular structures develop to form the basis for the constitution of a woven bone scaffold.² Signaling molecules will trigger the recruitment of osteogenic cells to either adhere to the implant surface (contact osteogenesis) or to line the pristine bony surface of the implant bed, thereby generating woven bone from the bony walls toward the implant (distance osteogenesis).

Controversy exists as to the necessity of close contact between the implant bed and the implant surface to guarantee successful osseointegration. In a recent histologic animal study, minimal osseointegration of implants placed into bony defects without primary bony contact of the implants was found.³ The gap between the implant bed and the surface was 1.2 mm. When the gap was limited to 0.7 mm, mineralized bone-to-implant contact developed, albeit to a reduced degree. This, in turn, confirmed the original

¹Assistant Professor, Department of Biomedical, Surgical and Dental Sciences, Università degli Studi di Milano, Italy.

²Postdoctoral Fellow, Ariminum Research and Dental Education Center (ARDEC), Rimini, Italy.

³Postdoctoral Fellow, Department of Biomedical, Surgical and Dental Sciences, Università degli Studi di Milano, Italy.

⁴Postdoctoral Fellow, University of Bologna, Italy.

⁵Adjunct Professor, Department of Biomedical, Surgical and Dental Sciences, Università degli Studi di Milano, Italy.

Correspondence to: Dr Daniela Carmagnola, Department of Biomedical, Surgical and Dental Sciences, Università degli Studi di Milano, Via Mangiagalli 31, 20133 Milan, Italy; fax: +390250315387; email:daniela.carmagnola@unimi.it

©2014 by Quintessence Publishing Co Inc.

studies on the critical jumping distance of bone being 0.5 mm.⁴⁻⁶

Therefore, it has to be assumed that only minimal gaps between the implant surface and the bony bed can exist if osseointegration is to develop. In a recent histologic animal study⁷ in which marginal bone defects of different sizes were produced around the implants (gaps of 0.5 mm and 1.25 mm), incomplete bone fill of the defects was reported after 30 days. On ground sections, a dense layer of connective tissue was detected on the implant surface that contained fibers running parallel and "attached" to the implant surface. This feature had already been identified previously in another experimental study in dogs.⁸

Bone healing around implants involves various processes and molecules. A recent literature review focusing on the role of osteopontin (OPN) on osseointegration pointed out that this molecule is a potent regulator of mineralization through different roles, such as opsonization of bone debris and enhancement of the osteoblastic activity.⁹

In the previously mentioned experiment by Rossi et al,⁷ paraffin sections were also prepared, on which immunohistochemical analysis was carried out. Consequently, it is the aim of the present study to report the histologic characteristics of the early phases of implant osseointegration, focusing on OPN concentrations in the coronal area of prepared marginal defects and in control sites without defect preparation.

Method and materials

The protocol was submitted and approved by the Ethical Committee for Animal Research of the University of the State of São Paulo, Brazil.

Surgical procedures were previously described.⁶ Briefly, 12 adult labrador dogs were used for the present experiment. During the surgical procedures, the animals were pre-anesthetized with Acepran (0.05 mg/kg, Univet-vetnil) and sedated with Zoletil (10 mg/kg, Virbac) and Xilazina (1 mg/kg, Cristália), complemented with ketamine (one-fourth of dose of 10 mg/kg, Cristália). Local anesthesia was provided at all surgical sessions. All mandibular premolars and first molars were extracted bilaterally in all dogs. Three months later, a crestal incision was performed in the premolar-molar region of the right side of the mandible. Full-thickness mucoperiosteal flaps were elevated to expose the edentulous alveolar ridges, and six sites were prepared for implant placement according to the manual of the implant system (Sweden & Martina, Due Carrare). Twist drills were used to prepare each recipient site for an implant 10 mm long and 3.3 mm in diameter (Premium, Sweden & Martina). Subsequently, specially designed step drills were used to widen the margins of the implant bed to 4.3 mm (small defects) at the two centrally located recipient sites and to 5.8 mm at the two distally located recipient sites (large defects). The two mesially located recipient sites (controls) were left without enlarge-

ment. Implants were subsequently placed with their margin flush with the buccal alveolar crest, and healing caps were screwed onto the implants. Following placement, a marginal gap occurred around the implants with defects (small defects = 0.5 mm; large defects = 1.25 mm). The flaps were sutured to allow a fully submerged healing. The timing of the experiments in the left sides and of sacrifices were planned in such a way as to obtain biopsy specimens representing healing times of 5, 10, 20, and 30 days. After surgery, the animals received Ketoflex 1% (0.02 mL/kg, Cetoprofeno, Biofarm Química e Farmaceutica) and Pentabiotico (Fort Dodge Animal Health). The animals were kept in kennels and on concrete runs at the university's field laboratory with free access to water and were fed with moistened balanced dog chow.

Postoperatively, the wounds were inspected daily for clinical signs of complications. Checkups were performed on a regular basis throughout the experiment. The animals were sacrificed with overdoses of thiopental (Cristalia).

Histologic preparation

The mandibles were removed and individual bone blocks containing the implant and the surrounding soft and hard tissues were fixed in 4% formaldehyde solution for 1 week. Of the six blocks for each healing time, three were processed for ground sectioning. These were analyzed for a previous study⁷ and

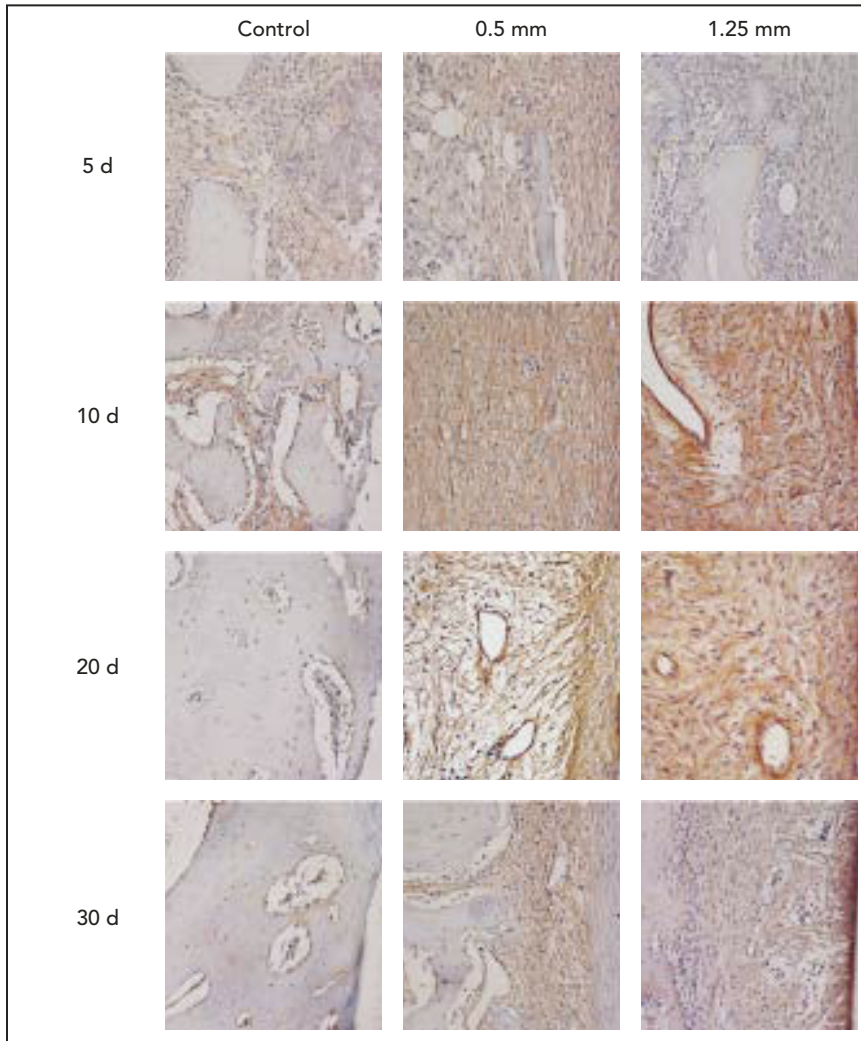


Fig 1 Immunohistochemical staining with osteopontin/hematoxylin revealing the OPN pattern in control, small (0.5 mm), and large (1.25 mm) defect samples at 5, 10, 20, and 30 days of healing.

were not considered for the present report. The remaining three blocks (control, small, and large defect) for each healing time were decalcified in ethylenediaminetetraacetic acid for 1 month, and, before the tissue was fully decalcified, incisions were made parallel with the long axis of the implants at the mesial and distal aspects of the biopsy specimens. Buccal and lingual portions of the peri-implant tissues were carefully

dissected, and one buccal and one lingual unit were prepared. Decalcification was completed and dehydration performed in increasing steps of ethanol concentrations. The units were then placed in xylol for 12 hours and infiltrated in paraffin overnight. The units were finally embedded in paraffin, and sections were produced from each tissue unit with the microtome (Leica Biosystems) set at 7 μ m. The sections

were stained with hematoxylin and eosin (Bio-Optica) to disclose the structures of the forming tissue and the presence of cellular infiltrate. Furthermore, picro-sirius red 1% (Sigma-Aldrich) staining was used to evaluate the distribution of the collagen fibers. From each tissue unit, six central sections were selected for histomorphometric analysis. The sections stained with picro-sirius red 1% were observed under polarized light to evaluate the birefringence of collagen. Immunohistochemical staining with osteopontin primary antibody was performed to assess the presence of OPN in the peri-implant tissues. Antigen retrieval was obtained using Proteinase K (Sigma-Aldrich) solution (1:50) at 37°C in a humidified chamber for 20 minutes. The slices were incubated with hydrogen peroxide to block endogen peroxidase for 5 minutes and then for 60 minutes at room temperature with anti-OPN primary antibodies (1:100) (anti-dog, in rabbit, Ana Spec). A large volume detection kit (Ultra-vision Quanto, Bio-Optica) was used to detect the primary antibody with a universal secondary antibody conjugated with a polymer linked to an enzyme that recognizes mouse immunoglobulins. The polymer complex was visualized using 3,3'-diaminobenzidine product as substrate system (Bio-Optica). Finally, the sections were counterstained with hematoxylin and mounted with Micromount (Bio-Optica).

The sections were observed using a light microscope (Eclipse E600, Nikon) equipped with a cali-

brated digital camera (DXM1200, Nikon). Morphometric measurements were carried out in the marginal coronal portion of the defect (an area 2.5 mm long and 0.25 mm wide adjacent to the implant) to quantify the proportion of blood vessels using a point-counting procedure with a 100 test point grid, at a magnification of $\times 200$. OPN was evaluated by quantifying the portion of the section colored with OPN immunohistochemical staining by means of an imaging program (Photoshop CS5, Adobe Systems) (Fig 1). The proportion of collagen was quantified under polarized light in the same fashion. For each parameter, mean values and SDs were calculated separately for the control, the small, and the large defects at 5, 10, 20, and 30 days, respectively (Fig 2).

The three groups were compared using the Kruskal-Wallis test, followed by post-hoc Mann-Whitney tests. Differences were considered statistically significant for $P < .017$.

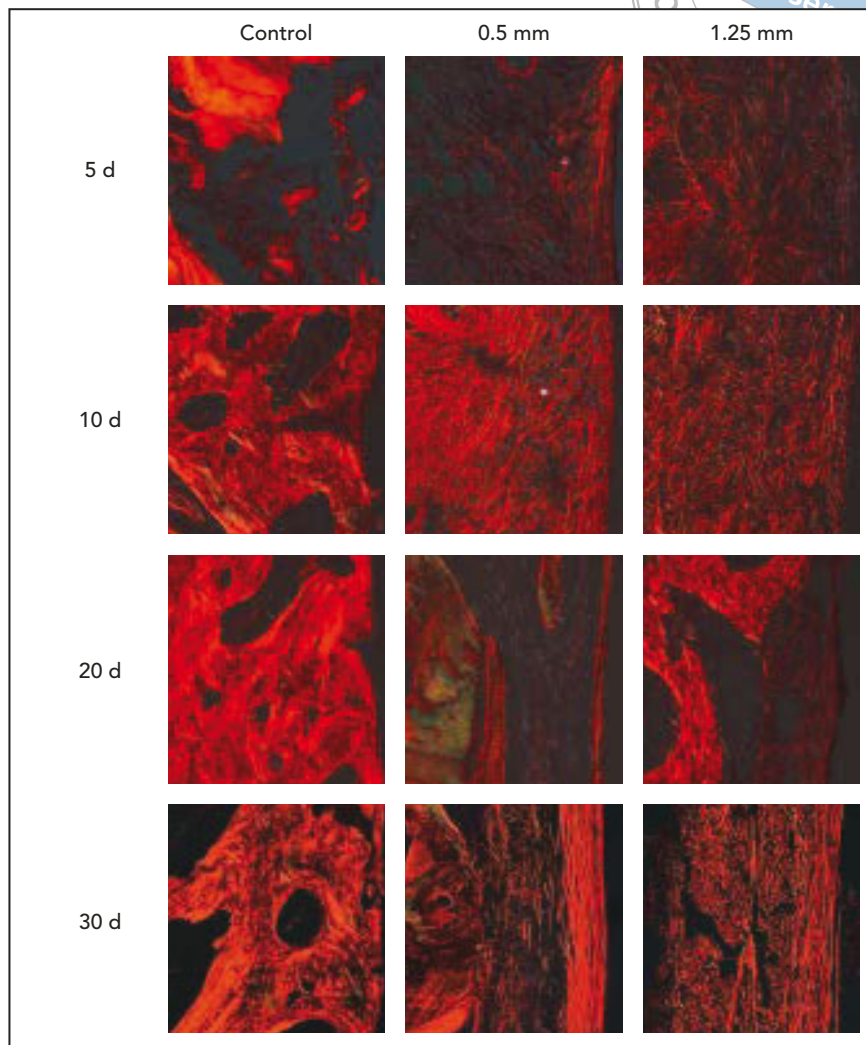


Fig 2 Birefringence of picro-sirius staining, revealing collagen bundle distribution in control, small (0.5 mm), and large (1.25 mm) defect samples at 5, 10, 20, and 30 days of healing (original magnification $\times 200$).

Results

All animals healed uneventfully, and all implants were integrated except for one control implant. During histologic processing, no artifacts occurred, nor were there any destroyed tissue blocks. Hence, all intervals of healing for the defects yielded a total of six sites. For the control defects, a total of six applied to all observation periods except for the 5-day specimens ($n = 5$).

Histologic evaluation

After 1 month of healing, the marginal defects were filled predominantly with newly formed bone, but only the basal portion of the implant was in close contact with bone. Bone debris was observed close to the implants at day 5 and was later replaced by collagen fibers and mineralized tissue.

Control defects

In the control samples, the peri-implant area was characterized by the presence of sparse collagen fibers between days 5 and 10, while woven bone in contact with the implant was later observed. The proportion of collagen fibers ranged from 9.52% at day 5 to 15.86% at day 20. Subsequently, it decreased slightly.

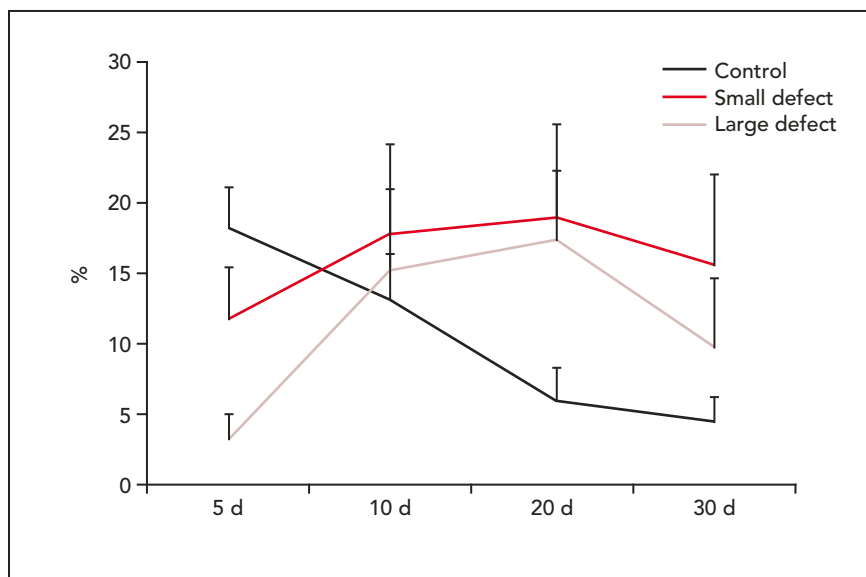


Fig 3 OPN concentration.

OPN was homogeneously distributed in the defect area. It showed its highest concentration at day 5 and then decreased continuously.

Overall, the proportion of blood vessels followed a similar trend in all groups. The vascularity increased in the first days and then decreased slightly. Control sites had the lowest proportion of blood vessels among groups at all times. This proportion increased rapidly from day 5 to day 20 and then decreased, ranging from 2.78% (day 5) to 3.01% (day 30).

Small defects

In the small defects, a layer of collagen fibers running parallel to the implant could be observed at day 10 that became denser and thicker with time. The space next to the defect, toward pristine bone, was occupied by sparse collagen fibers and at days 20 and 30 by miner-

alized tissue. The concentration of collagen fibers increased rapidly from day 5 to day 10, when it reached its maximum value. It decreased from day 10 to day 30.

OPN concentration increased slightly between days 5 and 20 and then decreased. OPN was distributed homogeneously at day 5, while at 20 days it was mainly concentrated adjacent to the implant, showing a decreasing gradient from the implant surface toward pristine bone. At day 30, OPN was mainly observed in the central area of the defect, ie, between the layer of tissue running parallel to the implant surface and the margin of pristine bone.

The small defects showed the highest proportions of blood vessels at all times, ranging from 6.02% (day 30) to 6.68% (day 20). Blood vessels increased from day 5 to day 10 and then decreased slightly.

Large defects

In the large defects, the collagen fibers had a similar distribution as in the small defects, but the formation of a bundle of collagen fibers running parallel to the implant seemed less pronounced. Mineralized tissue was observed in the defect area at day 30. Collagen fiber concentration was the lowest among groups and increased continuously from day 5 to day 30.

In the small defects, OPN showed a gradient from the implant surface toward the pristine bone, but in the large defects OPN was observed later and had slightly lower concentrations. It was distributed homogeneously in the defect area between 5 and 20 days. At 30 days, it was mainly observed in the central area of the defect, ie, between the layer of tissue running parallel to the implant surface and the margin of pristine bone.

In the large defects, blood vessels increased slightly from 5 to 10 days and then remained stable.

Statistical analysis

OPN

The control sites had statistically significant differences in OPN compared with small and large defects at 5 ($P < .05$ and $P < .01$, respectively) and 20 days ($P < .05$ and $P < .01$, respectively) and compared with small defects only at 30 days ($P < .01$). On the other hand, the large and small defects had a statistically significant difference only at day 5 (Fig 3).

Collagen

Statistically significant differences were observed between the control sites and large defects at days 5 ($P < .01$), 10 ($P < .05$), and 20 ($P < .01$). A statistically significant difference between small and large defects was found only at day 10 ($P < .01$) (Fig 4).

Vessels

A statistically significant difference was observed only at day 5 between control sites and small defects ($P < .01$) (Fig 5).

Discussion

As previously reported,⁷ implants placed in a conventional way and in marginal defects of 0.5 and 1.25 mm resulted in adequate bone fill and partial osteointegration after 30 days. In this report, some characteristics of the process of bone healing at controls and small and large defects are described.

Comparing the results among the three experimental groups, conventionally placed implants showed the highest concentration of collagen, the lowest proportion of vessels, and decreasing levels of OPN through time. The collagen fibers were not strictly organized in a bundle running parallel to the implant length. OPN was easily detectable from day 5 and was evenly spread in peri-implant tissue. The small defects showed the highest proportion of blood vessels and increasing levels of OPN from day 5 to day 30. The collagen fibers were organized in a thick bundle

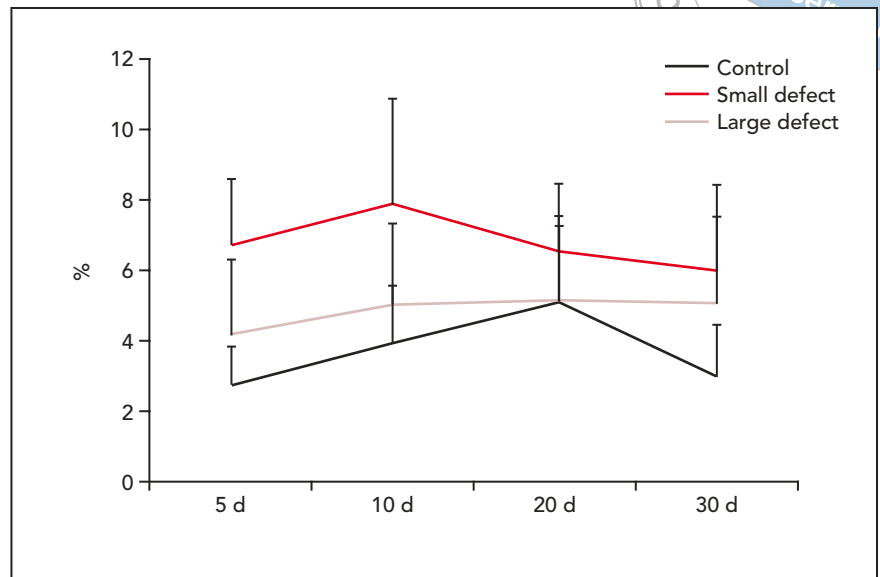


Fig 4 Collagen concentration.

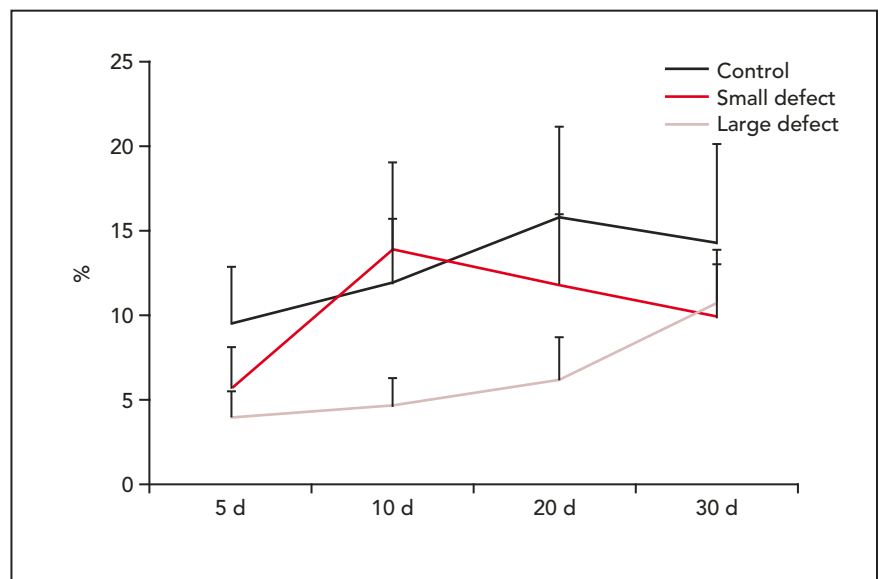


Fig 5 Vessels concentration.

facing the implant and running in an apicocoronal direction. OPN was more concentrated close to the implant, in the collagen bundle area, and gradually decreased toward pristine bone. The large defects had features similar to those of the small defects, though with lower concentrations of blood ves-

sels, collagen, and OPN. It has to be underlined that the measurements were carried out in a standardized coronal peri-implant area 2.5 mm long and 0.25 mm wide, therefore including the pristine bone in the conventionally placed implants and the gap in the small- and large-defect groups.

It is known that osseointegration of rough titanium implants proceeds through different phases: the blood clot and bone debris produced during drilling are quickly replaced with provisional connective tissue that is remodeled and in time results in mineralized tissue and marrow spaces.^{2,10}

In a canine experiment by Berglundh et al,¹¹ the authors observed that during the first 2 to 3 weeks of peri-implant healing, there is an increase in blood vessel density, followed by a plateau. Similar results were observed in the present experiment. In all groups, blood vessel concentration increased in the first 2 to 3 weeks and either became stable or decreased later. The fact that the sites with marginal defects showed higher concentrations of blood vessels compared to control sites might be explained by the need for a larger blood supply to quickly fill the peri-implant gaps in the first phases of healing.

In the present study, conventional sites harbored the highest concentrations of collagen. The fibers were observed in the narrow space between pristine bone and implant, ran in different directions, and were quickly replaced by mineralized tissue. In contrast, the collagen fibers in the small defects were organized in a layer that ran parallel to the implant at day 10 and became denser and thicker with time. In the large defects, the collagen fibers had a similar distribution as in the small defects, though the formation of a collagen bundle appeared less pronounced.

In the most coronal portion of titanium implants, at the abutment level, collagen fibers have to provide a functional seal not only in the early phases of wound healing, but also, since cementum does not form around implants, in later phases to protect the area from bacterial invasion.¹² Many authors have described the presence of longitudinal and circumferential fibers around conventionally placed implants.¹³ It has been shown that collagen fiber organization and distribution depend on the challenges that the implant has to cope with. With time, the fibers' organization may vary depending on the load and forces that the implants have to withstand.¹⁴ In this study, the implants were not loaded. The differences concerning the fibers' organization around conventionally placed implants and implants with marginal gaps might therefore be explained by the fact that where the gap between implant and pristine bone is larger, a thicker and denser collagen seal is required to prevent bacterial invasion while the gap gets filled. In such circumstances, collagen fibers may need (and have the time) to become organized, seal, and fill the area while the processes of distance and contact osteogenesis are preparing to occur.

OPN is a versatile protein involved in diverse biologic processes whose precise functions are still being explored.¹⁵ It has been studied widely in bone fracture healing, a process that involves a complex sequence of biologic events orchestrated by a variety of growth

factors and proteins. OPN is one of the major extracellular matrix proteins present in bone and in a number of nonmineralized tissues and plays a functional role in controlling bone mineralization, bone remodeling, and angiogenesis. In a study in wildtype and OPN(-/-) mice,¹⁶ OPN deficiency was found to delay but not prevent bone regeneration and remodeling of fractures. The authors concluded that: "OPN deficiency alters the functionality of multiple cell types, resulting in delayed early vascularization, altered matrix organization and late remodeling, and reduced biomechanical properties." OPN is coexpressed in various cell types with another extracellular matrix protein, bone sialoprotein (BSP), and both are actively involved in bone deposition and remodeling. Studies on OPN- and BSP-deficient mice have shown that BSP, but not OPN, plays a role in primary bone formation and mineralization of newly formed bone during the process of cortical bone healing.¹⁷ OPN deficiency in healthy mice does not affect bone turnover and mineralization. However, the response to pathologies such as tissue injury, inflammation, infection, and autoimmune disorders differs between wildtype mice and OPN(-/-) mice in the sense that OPN-deficient mice appear to be protected from some autoimmune disorders and inflammatory conditions but are more susceptible to some infections.¹⁸

OPN's role in peri-implant healing has been recently described by McKee et al.⁹ Following bone drill-

ing and inflammatory response, macrophages appear and secrete OPN. OPN binds and coats all mineralized surfaces, both to promote cement line formation on the bone wound margins and to clear bone debris (by opsonization). Concerning osteoblasts' activity, OPN contributes to cell adhesion, cell signaling, and matrix mineralization, leading to the integration of new bone into preexisting bone. In the present experiment, OPN was evenly distributed in the peri-implant tissue at control sites, where it showed higher concentrations in the early phases of bone healing and decreased with time. Such findings may suggest that in conventionally placed implants, OPN works at the same time on clearance and bone formation. On the other hand, the finding that OPN was mainly located in the collagen bundle section of the peri-implant tissue around the implants placed into the defects and its increasing concentrations with time might indicate that OPN is mainly needed close to the implant when a large gap is present. Therefore, OPN appears to promote both distance osteogenesis and contact osteogenesis by acting as an adhesion molecule for the osseous filling process from the native bone and by preparing the tissue-lining implant for mineralization.

Acknowledgments

The authors reported no conflicts of interest related to this study.

References

1. Davies JE. Mechanisms of endosseous integration. *Int J Prosthodont* 1998;11:391-401.
2. Abrahamsson I, Berglundh T, Linder E, Lang NP, Lindhe J. Early bone formation adjacent to rough and turned endosseous implant surfaces. An experimental study in the dog. *Clin Oral Implants Res* 2004;15:381-392.
3. Sivolella S, Bressan E, Salata LA, Urrutia ZA, Lang NP, Botticelli D. Osteogenesis at implants without primary bone contact - an experimental study in dogs. *Clin Oral Implants Res* 2012;23:542-549.
4. Johner R. Dependence of bone healing on defect size. *Helv Chir Acta* 1972;39:409-411.
5. Schenk RK, Willenegger HR. Histology of primary bone healing: Modifications and limits of recovery of gaps in relation to extent of the defect. *Unfallheilkunde* 1977;80:155-160.
6. Botticelli D, Berglundh T, Buser D, Lindhe J. The jumping distance revisited. *Clin Oral Implants Res* 2003;14:35-42.
7. Rossi F, Botticelli D, Pantani F, Pereira FP, Salata LA, Lang NP. Bone healing pattern in surgically created circumferential defects around submerged implants: An experimental study in dog. *Clin Oral Implants Res* 2012;23:41-48.
8. Botticelli D, Berglundh T, Buser D, Lindhe J. Appositional bone formation in marginal defects at implants. *Clin Oral Implants Res* 2003;14:1-9.
9. McKee MD, Pedraza CE, Kaartinen MT. Osteopontin and wound healing in bone. *Cells Tissues Organs* 2011;194:313-319.
10. Carmagnola D, Abati S, Addis A, et al. Time sequence of bone healing around two implant systems in minipigs: Preliminary histologic results. *Int J Periodontics Restorative Dent* 2009;29:549-555.
11. Berglundh T, Abrahamsson I, Welander M, Lang NP, Lindhe J. Morphogenesis of the peri-implant mucosa: An experimental study in dogs. *Clin Oral Implants Res* 2007;18:1-8.
12. Çomut AA, Weber HP, Shortkroff S, Cui FZ, Spector M. Connective tissue orientation around dental implants in a canine model. *Clin Oral Implants Res* 2001;12:433-440.
13. Schupbach P, Glauser R. The defense architecture of the human periimplant mucosa: A histological study. *J Prosthet Dent* 2007;97:S15-S25.
14. Traini T, Degidi M, Caputi S, Strocchi R, Di Iorio D, Piattelli A. Collagen fiber orientation in human peri-implant bone around immediately loaded and unloaded titanium dental implants. *J Periodontol* 2005;76:83-89.
15. Standal T, Borset M, Sundan A. Role of osteopontin in adhesion, migration, cell survival and bone remodeling. *Exp Oncol* 2004;26:179-184.
16. Duvall CL, Taylor WR, Weiss D, Wojtowicz AM, Guldberg RE. Impaired angiogenesis, early callus formation, and late stage remodeling in fracture healing of osteopontin-deficient mice. *J Bone Miner Res* 2007;22:286-297.
17. Monfoulet L, Malaval L, Aubin JE, et al. Bone sialoprotein, but not osteopontin, deficiency impairs the mineralization of regenerating bone during cortical defect healing. *Bone* 2010;46:447-452.
18. Rittling SR. Osteopontin in macrophage function. *Expert Rev Mol Med* 2011;13:e15.